Gabor deconvolution

Gary F. Margrave* - Geology and Geophysics and Michael P. Lamoureux - Mathematics and Statistics, University of Calgary

Summary

We present a novel approach to nonstationary seismic deconvolution based upon the Gabor transform. The latter is based upon the quantum mechanical idea that a signal can be represented in terms of sinusoids that are modulated by translated Gaussian windows. The resulting time-frequency decomposition is an suite of local Fourier transforms which displays any nonstationary spectral trends, and where the interrelationship between individual transforms is well-understood.. In a result that generalizes the seismic convolutional model, we show that the Gabor transform of a nonstationary seismic signal is given by the product of source signature, Q filter, and reflectivity effects. We then use this spectral factorization theorem as a basis for a new deconvolution algorithm in the Gabor domain. Essentially, we estimate the Gabor spectrum of the underlying reflectivity directly from the Gabor spectrum of an attenuated seismic signal. Tests on synthetic and real data show that our method works well and combines the effects of source-signature inversion and a data-driven inverse Q filter. In comparison with a stationary Wiener deconvolution, our Gabor deconvolution is similar within the Wiener design gate and superior elsewhere.

Introduction

In 1946, Dennis Gabor, the inventor of the hologram, proposed the expansion of a wave in terms of Gaussian wave packets. An example of such a wave packet is a sine wave multiplied by a Gaussian function. If a signal is modulated (multiplied) by a Gaussian window of a certain width and central time, then a Fourier expansion of the modulated signal gives a measure of the local spectrum. Clearly such a spectrum is not unique since the width of the Gaussian is arbitrary; but nevertheless, such local spectra are extremely useful. If a collection of local spectra is computed for a suite of window positions, the result is a time-frequency decomposition called a Gabor transform. Furthermore, if the signal can be reconstructed from this decomposition, then a nonstationary filter can be achieved by modifying the decomposition before reconstruction.

In this paper we present the theory of the continuous Gabor transform and only an approximate theory for the discrete transform. The modern theory of the discrete Gabor transform is usually attributed to Bastiaans (1980). A complete overview of the theory of the discrete Gabor transform is found in Feichtinger and Strohmer (1998). Our approximate discrete transform does not exactly recreate the original signal but the loss can be made as small as desired. Next, we apply the continuous Gabor transform to a mathematical model of a nonstationary seismogram to show how the Gabor spectrum factors into wavelet, Q filter, and reflectivity components. Finally, we use these tools to develop a seismic deconvolution algorithm that is a direct extension of standard (e.g. Wiener) methods to the nonstationary case. The resulting minimum-phase deconvolution technique simultaneously accomplishes the tasks of source waveform inversion and (apparent) inverse Q filtering.

The Gabor transform

Following Mertins (1999), we define the continuous Gabor transform of a signal s(t) as

$$\overset{\backslash}{s}(\tau, f) = \int_{-\infty}^{\infty} s(t) g(t-\tau) e^{-2\pi i f t} dt \qquad (1)$$

where $g(t)$ is the *Gabor analysis window* and τ is the location of the window center. Although we use $g(t)$ as a Gaussian function, the theory works well for quite general windows including Dirac delta distributions. Given $\overset{\backslash}{s}(\tau, f)$, the signal can be reconstructed from the expression

$$s(t) = \int_{-\infty}^{\infty} \int_{-\infty}^{\infty} \overset{\backslash}{s}(\tau, f) \gamma(t-\tau) e^{2\pi i f t} df d\tau \qquad (2)$$

where $\gamma(t)$ is the *Gabor synthesis window*. The analysis and synthesis windows must satisfy the condition

$$\int_{-\infty}^{\infty} g(t)\gamma(t) dt = 1 . \qquad (3)$$

Given equation (1) and the condition (3), the derivation of equation (2) is straightforward and can be found in Mertins(1999).

Though the discrete Gabor transform can be formulated as a lossless process, we choose a simpler, approximate approach. Our approximation relies upon a special property of Gaussians that links the Gaussian width with the spacing between Gaussians. That is, it is possible to choose a set of Gaussians such that

$$h(t) \equiv \sum_{k \in \mathbb{C}} g(t - k\Delta\tau) \approx 1 \qquad (4)$$

where

$$g(t - k\Delta\tau) = \frac{\Delta\tau}{T\sqrt{\pi}} e^{-[t-k\Delta\tau]^2 T^{-2}} \qquad (5)$$

with T being the Gaussian (half) width. More precisely, it can be shown that

$$\sum_{k \in \mathbb{C}} g(t - k\Delta\tau) = 1 + 2\cos(2\pi t/\Delta\tau) e^{-[\pi T/\Delta\tau]^2} + L \qquad (6)$$

Here the second term estimates the error (all remaining terms are exponentially smaller) in the approximation. Thus the error can be made arbitrarily small by increasing the ratio $T/\Delta\tau$. The maximum error is –21 decibels for $T/\Delta\tau = .5$, -85 decibels for $T/\Delta\tau = 1$, -150 decibels for $T/\Delta\tau = 1.5$ and -340 decibels $T/\Delta\tau = 2$. Thus for $T/\Delta\tau > 1.5$, the error is negligible for most geophysical purposes.

Using relation (4) as an equality, we decompose a seismic signal into Gaussian slices as

$$s(t) = s(t) \sum_{k \in \mathbb{C}} g(t - k\Delta\tau) = \sum_{k \in \mathbb{C}} s(t) g(t - k\Delta\tau) = \sum_{k \in \mathbb{C}} s_k(t) \qquad (7)$$

where the Gaussian slice is $s_k(t) = s(t) g(t - k\Delta\tau)$. Next we apply a forward Fourier transform

$$\hat{s}(f) = \sum_{k \in \mathbb{C}} \int_{-\infty}^{\infty} s_k(t) e^{-2\pi i f t} dt = \sum_{k \in \mathbb{C}} \mathbf{H}_k(f) \qquad (8)$$

where $\hat{s}$ is the Fourier transform of s and

$$\mathbf{H}_k(f) \equiv \int_{-\infty}^{\infty} s_k(t) e^{-2\pi i f t} dt \qquad (9)$$

is our approximate Gabor transform. As written, it is discrete in the window position coordinate, as indexed by *k*, but continuous in frequency *f*. Of course, in a computer implementation, we would replace the integral Fourier transform with the DFT.

The recovery of the original signal follows by simply taking the inverse Fourier transform of equation (9)

$$s(t) = \int_{-\infty}^{\infty} \left[\sum_{k \in \mathbb{C}} \mathbf{H}_k(f) \right] e^{2\pi i f t} df . \qquad (10)$$

Thus the discrete Gabor transform is simply summed over *k* and then inverse Fourier transformed. Figure 1 shows a synthetic seismic signal and the result of running that signal through the forward and inverse Gabor transform, with no processing in the

Gabor domain. The signal is recreated with excellent fidelity except for a slight amplitude loss at either end. This end effect persists about one Gaussian width ($2T$) from each end (.2 seconds in this case). The actual magnitude of the end effect has been reduced in this example by the simple normalization procedure

$$\tilde{H}_k(f) \equiv h^{-1}(k\Delta\tau) \int_{-\infty}^{\infty} s_k(t) e^{-2\pi i f t} dt \qquad (11)$$

where $h(t)$ is given by equation (4).

Gabor factorization of a nonstationary trace model

We now present a trace model that includes the source waveform and the nonstationary effects of dissipation as predicted by the constant-Q model though it does not explicitly model stratigraphic filtering. First we consider the effect of constant Q and model it as

$$s_Q(t) = \int_{-\infty}^{\infty}\int_{-\infty}^{\infty} \alpha_Q(\tau,f) r(\tau) e^{2\pi i f[t-\tau]} d\tau df \qquad (12)$$

where $r(\tau)$ is the reflectivity sequence and the constant-Q transfer function is

$$\alpha_Q(\tau,f) = e^{-\pi f \tau/Q + iH(\pi f \tau/Q)} \qquad (13)$$

where H denotes the Hilbert transform over f at constant τ. Equation (12) can be understood as a nonstationary convolution by noting that the f integral can be written as

$$a_Q(\tau, t-\tau) = \int_{-\infty}^{\infty} \alpha_Q(\tau,f) e^{2\pi i f[t-\tau]} df \qquad (14)$$

so that

$$s_Q(t) = \int_{-\infty}^{\infty} a_Q(\tau, t-\tau) r(\tau) d\tau \qquad (15)$$

which is a nonstationary convolution filter as defined by Margrave (1998).

As defined by equation (12), s_Q models dissipation for an impulsive source. We simply apply a more general source signature with a stationary convolution and write our final nonstationary trace model as

$$\hat{s}(f) = \hat{w}(f) \int_{-\infty}^{\infty} \alpha_Q(\tau,f) r(\tau) e^{-2\pi i f \tau} d\tau \qquad (16)$$

where $\hat{w}$ and $\hat{s}$ are the Fourier transforms of the source signature and the nonstationary seismic trace respectively. Equation (16) is a replacement for the familiar stationary convolution model. We prefer to express it in the Fourier domain for simplicity. The attenuated signal of Figure 1 was generated using this equation with $Q = 25$ and $\hat{w}(f)$ specifying a minimum phase source signature with a dominant frequency of 20 Hz.

We have derived an asymptotic result for the Gabor transform of $s(t)$, whose Fourier transform is given by equation (16), as

$$\check{s}(\tau,f) \approx \hat{w}(f) \alpha_Q(\tau,f) \check{r}(\tau,f) \qquad (17)$$

where the $\approx$ sign means that this is the leading term in an asymptotic series. (Space does not permit us to include our derivation here but we will provide the details upon request.) In words, the Gabor transform of our nonstationary trace is approximately equal to the product of the Fourier transform of the source signature, the constant Q transfer function, and the Gabor transform of the reflectivity. Since, for fixed τ, the Gabor transform is just a Fourier transform, this is a *temporally local* convolutional model.

Figure 2 shows the magnitude of the Gabor transform of the attenuated signal of Figure 1. It was computed with $T = 0.1$ s and $\Delta\tau = 0.01$ s. In Figure 3 is the Gabor magnitude spectrum of the random reflectivity series used to generate the synthetic signal of Figure 1. Figure 4 shows the magnitude of the constant-Q attenuation surface ($|\alpha_Q(\tau,f)|$) and Figure 5 displays $|\hat{w}(f)|$ as an invariant function of time. The product of the spectra of Figures 3, 4, and 5 is the model expressed by equation (17) and is shown in Figure 6. Comparison with Figure 2 suggests the model is quite effective in this case.

A Gabor deconvolution algorithm

We propose a method of deconvolution that estimates the Gabor transform of the reflectivity from the Gabor transform of a nonstationary seismic trace. From equation (17), this amounts to dividing the Gabor spectrum of the seismic trace by estimates of the source waveform and the Q transfer function. As with stationary deconvolution, this is an inherently nonunique *spectral factorization* problem that requires assumptions about the three components of the right side of equation (17). From the outset, we will work only with the magnitude of equation (17) and, when an estimate of $|\hat{w}(f)||\alpha_Q(\tau,f)|$ (we call this the spectrum of the propagating wavelet) is available, a minimum-phase function will be calculated for it. We assume that $|\check{r}(\tau,f)|$ is a rapidly varying function in both variables as is seen in our example in Figure 3. In contrast, $|\hat{w}(f)|$ is assumed to be independent of τ and smoothly varying in f while $|\alpha_Q(\tau,f)|$ is an exponential decay surface in both variables (see Figures 4 and 6).

The simplest Gabor deconvolution algorithm estimates $|\hat{w}(f)||\alpha_Q(\tau,f)|$ by smoothing $|\check{s}(\tau,f)|$ by convolving over (τ,f) with a 2D boxcar. Often this is a surprisingly good estimate though it is strongly dependent upon the dimensions of the boxcar. There are many variations on this basic method such as using smoothers of different shapes (triangles or Gaussians for example). The basic drawback to the smoothing approach is that it will always result in a biased estimate of $|\hat{w}(f)||\alpha_Q(\tau,f)|$. To see this, suppose we have an extremely lucky case where $|\check{r}(\tau,f)|$ so that $|\check{s}(\tau,f)|$ is already equal to $|\hat{w}(f)||\alpha_Q(\tau,f)|$. Then, because the smoother will always alter the function to which it is applied, we obtain the wrong answer.

Many other spectral factorization methods are possible. Grossman et al. (2002) show how the model of equation (17) can be imposed on a measured Gabor spectrum by least squares, thereby obtaining estimates of Q and $|\hat{w}(f)|$. Iliescu and Margrave (2002) compare simple spectral smoothing with a 2D boxcar to smoothing along curves $\tau f = \text{constant}$. In any case, let $|\check{\sigma}(\tau,f)|$ symbolize a suitably smooth approximation to $|\check{s}(\tau,f)|$ such that it is an acceptable estimation of $|\hat{w}(f)||\alpha_Q(\tau,f)|$. Then we calculate a phase function via a Hilbert transform as

$$\varphi(\tau,f) = \int_{-\infty}^{\infty} \frac{\ln|\check{\sigma}(\tau,f')|}{f - f'} df' \qquad (18)$$

where we assume that $|\check{\sigma}(\tau,f)|$ has been designed to have no zeros. Given $|\check{\sigma}(\tau,f)|$ and the phase from equation (18) it is a simple matter to calculate $\check{\sigma}(\tau,f)$ and estimate the Gabor spectrum of the reflectivity as

$$\check{r}(\tau,f)_{est} = \frac{\check{s}(\tau,f)}{\check{\sigma}(\tau,f)}. \qquad (19)$$

Examples

Figure 7 shows a smoothed rendition of Figure 2 that we take as a suitable estimate of $|\hat{w}(f)||\alpha_Q(\tau,f)|$. In this case, smoothing in f was accomplished by computing a Burg spectral estimate (Claerbout, 1976) corresponding to the Fourier estimate in Figure 2. Then smoothing in τ was done by convolution with a boxcar of length 0.1 seconds. Then dividing the spectrum of Figure 2 by that of Figure 7 and applying a stationary filter to reject frequencies above 125 Hz gives the estimate of the Gabor spectrum of the reflectivity shown in Figure 8. Comparison with Figure 3 shows that the estimate is quite good. Figure 9 shows the Gabor spectrum of the attenuated signal after it has been processed more conventionally with AGC and Wiener deconvolution. The Wiener design gate was from 0.35 to 0.65 seconds. This shows the familiar behavior that the Wiener operator over whitens data at earlier times.

Figure 10 compares the Gabor deconvolution result with several other traces in the time domain. The Gabor result matches the bandlimited reflectivity very well and has a much whiter and more stationary appearance than the AGC+Wiener result. The Fourier amplitude spectra of these traces are shown in Figure 11. Again there is a good correlation between the Gabor result and bandlimited reflectivity while the Weiner result is less similar.

Figures 12 and 13 compare Gabor deconvolution with conventional Wiener deconvolution on a real seismic shot record. The Wiener design gate was from 1.0 to 1.6 seconds and within this zone the results are superficially similar. However, a detailed inspection shows phase and amplitude differences and a different response to ground roll. Also apparent is that the Wiener result is dramatically inferior to Gabor above the design gate.

Conclusions

We have described the Gabor transform in both continuous and discrete forms. Using a simplified nonstationary trace model, we derived a spectral factorization in the Gabor domain that is the basis for our deconvolution procedure. Our Gabor deconvolution estimates the propagating wavelet spectrum by smoothing the magnitude of the Gabor spectrum of the seismic trace. Phase is calculated by a minimum phase assumption. Finally reflectivity is estimated by dividing the Gabor spectrum of the seismic trace by the estimate of the propagating wavelet. Our examples show that this new technique works well, usually giving better results than a conventional approach using Wiener deconvolution.

Acknowledgements

References

Bastiaans, M. J., 1980, Gabor's expansion of a signal into Gaussian elementary signals: Proceedings of the IEEE, **68**, 538-539.

Claerbout, J. F., 1976, Fundamentals of Geophysical Data Processing: McGraw-Hill.

Feichtinger, H. G., and Strohmer, T., 1998, Gabor analysis and algorithms: Theory and applications: Birkhauser, ISBN 0-8176-3959-4.

Gabor, D., 1946, Theory of communication: J. IEEE (London), **93(III)**, 429-457.

Grossman, J. P., Margrave, G. F., Lamoureux, M. P., and Aggarwala, R., 2002, Constant-Q wavelet estimation via a Gabor spectral model: CSEG Convention Expanded Abstracts.

Iliescu, V., and Margrave, G. F., 2002, Reflectivity amplitude restoration in Gabor deconvolution: CSEG Convention Expanded Abstracts.

Margrave, G. F., 1998, Theory of nonstationary linear filtering in the Fourier domain with application to time-variant filtering: Geophysics, **63**, 244-259.

Mertins, A., 1999, Signal Analysis: John Wiley and Sons, ISBN 0-471-98626-7.

Schoepp, A. R., and Margrave, G. F., 1998, Improving seismic resolution with nonstationary deconvolution: 68th Annual SEG meeting, New Orleans, La.

Figures
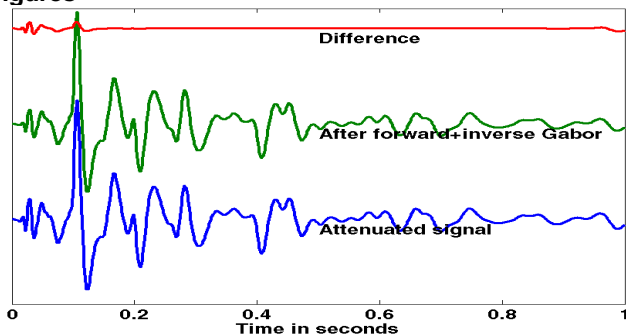
Figure 1. A synthetic seismogram with attenuation (bottom) is shown after a forward and inverse Gabor transform (middle) and the difference is on top.
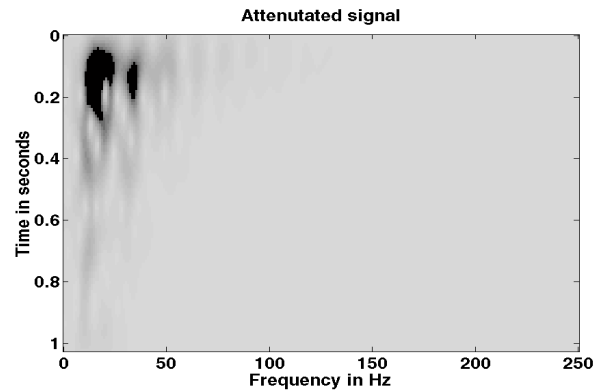
Figure 2. The Gabor (magnitude) spectrum of the attenuated signal of Figure 1. Darker shading indicates greater values.
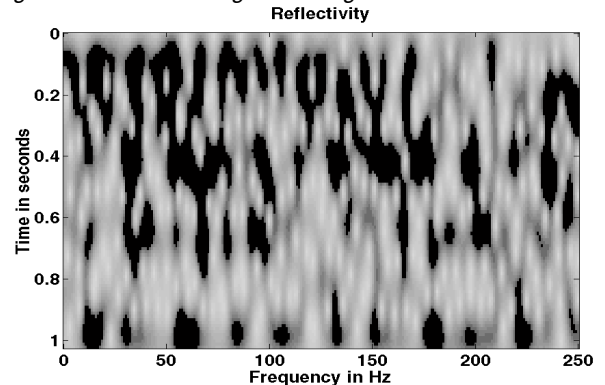
Figure 3. The Gabor (magnitude) spectrum of the reflectivity used to make the attenuated signal of Figure 1.
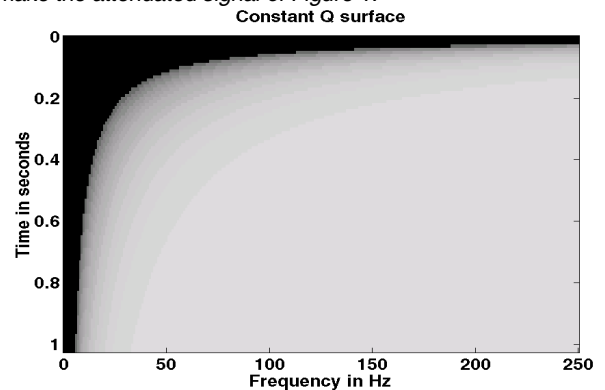
Figure 4. The magnitude of the constant Q attenuation surface.
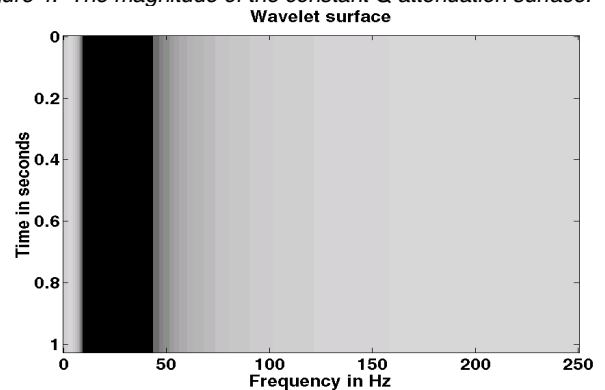
Figure 5. The magnitude of the source-signature surface.
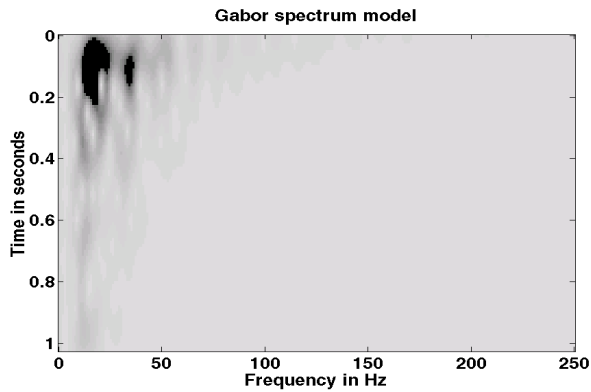
Figure 6. The product of the time-frequency surfaces of Figures 3-5. This is a model for the actual Gabor spectrum of Figure 2.
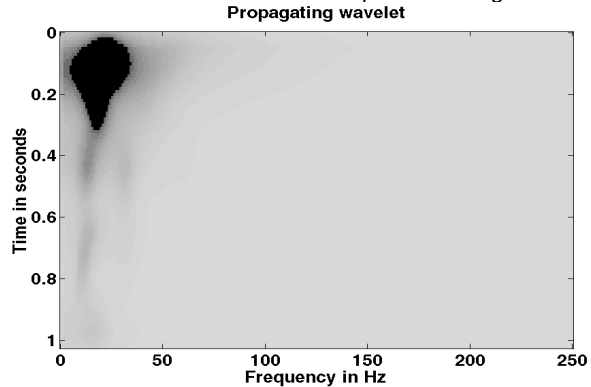
Figure 7. The estimate of the "propagating wavelet" spectrum derived by smoothing the Gabor (Burg) spectrum corresponding to Figure 2.
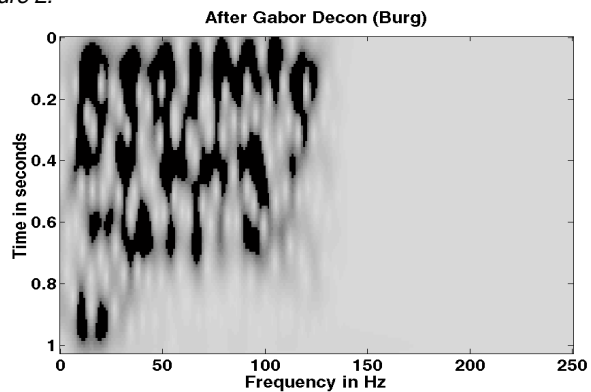
Figure 8. The result of dividing the Gabor spectrum in Figure 2 by that in Figure 7. This is the estimate of the Gabor spectrum of the reflectivity. Compare with Figure 3. A stationary highcut filter has been applied to reject frequencies above 125 Hz.
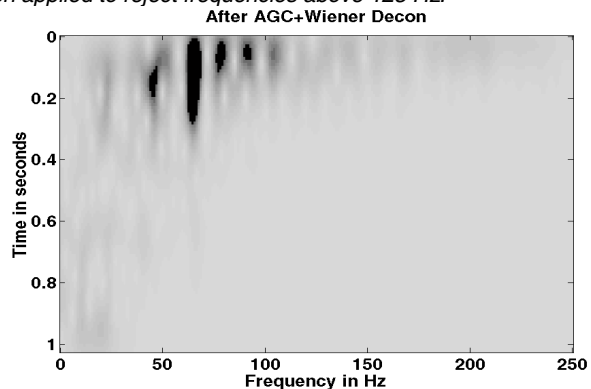
Figure 9. The Gabor spectrum of the result of performing AGC followed by Wiener deconvolution of the attenuated signal of Figure 1. This is the Gabor spectrum of the trace shown in Figure 10.
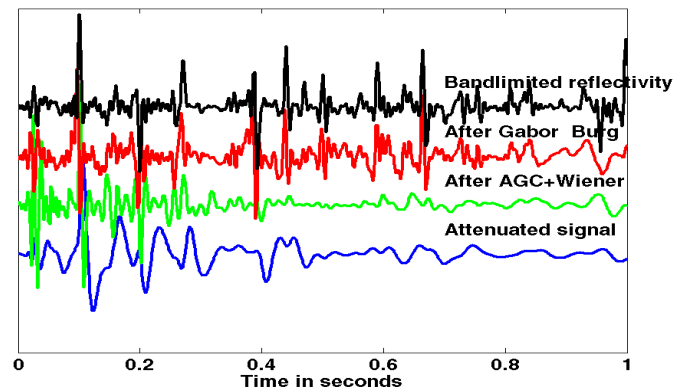
Figure 10. The attenuated signal of Figure 1 is shown (bottom) compared with a conventional AGC->Wiener deconvolution (second) and a Gabor/Burg deconvolution (third) and finally a bandlimited reflectivity (top). The reflectivity and the Gabor deconvolution have been bandlimited to less than 125 Hz.
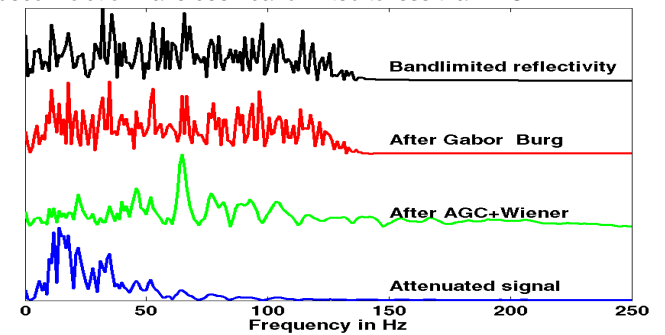
Figure 11. The Fourier spectra (entire trace) of the signals in Figure 10.
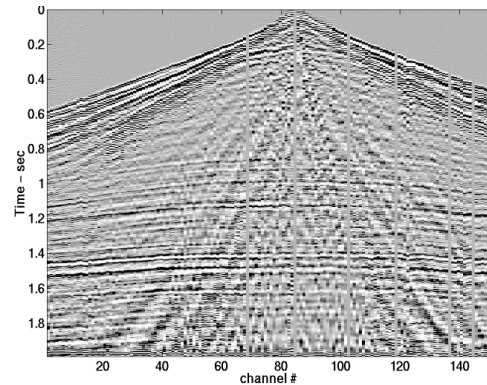
Figure 12. A seismic shot record processed with Gabor deconvolution.
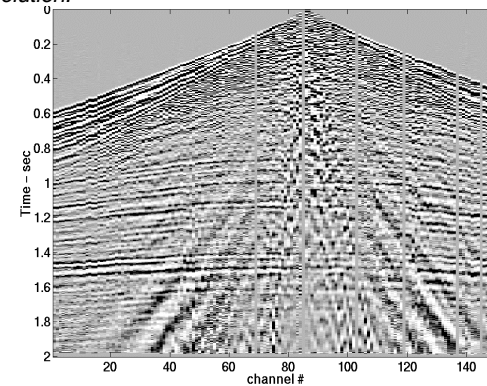
Figure 13. The same seismic shot record as Figure 12 processed with exponential gain and Wiener deconvolution.